

# Theoretical assessment of the Ni–Sn system

Adela Zemanova · Ales Kroupa · Alan Dinsdale

Received: 22 February 2012 / Accepted: 22 April 2012  
© Springer-Verlag 2012

**Abstract** A new theoretical assessment of the Ni–Sn system has been performed by use of the CALPHAD method. Recent experimental results were significantly different from older experimental data and, therefore, a new reassessment of older theoretical work was necessary. The theoretical models for some intermetallic phases were changed to make them consistent with other binary systems in the thermodynamic database developed in the scope of COST action MP0602. Very good agreement was reached both with new experimental phase equilibrium data and older thermodynamic data.

**Keywords** Ni–Sn phase diagram · CALPHAD method · Theoretical assessment

## Introduction

Significant changes have occurred in the electronics industry over the last 10 years in connection with the transfer to lead-free soldering. As a result of these changes, detailed understanding of the behaviour of new materials is necessary. One crucial system associated with this new

technology is the Ag–Cu–Ni–Sn system. Its importance results from the composition of the most common lead-free solder for mainstream applications (Sn–Ag–Cu alloy) in conjunction with Ni as substrate material.

The Ni–Sn system is an important basic subsystem of the system mentioned above. It is important both for traditional and lead-free soldering, and its detailed understanding is also particularly important in new technology, e.g., transient liquid bonding [1, 2]. This technology has been studied intensively in connection with the development of materials for high-temperature lead-free soldering and Cu–Ni–Sn alloys are possible candidates. Therefore, knowledge of the phase diagram of the Ni–Sn system is very important from the perspective of the development of new soldering materials or new joining technology.

Theoretical modelling of phase diagrams and the thermodynamic properties of complex systems has proved to be essential in materials science, and the CALPHAD method, especially, is now used extensively in research in both industrial and academic environments as very efficient tool for new material development. The possibility of modelling the phase diagrams and thermodynamic properties of complex alloys by use of robust, high-quality theoretical descriptions of simple systems enables significant saving of time and money in the design of new promising alloys and limits the need for extensive experimental work.

The Ni–Sn system has been theoretically assessed several times by use of the CALPHAD method, but new experimental information published recently by Schmetterer et al. [3] has necessitated complete reassessment of the system. The first assessment of this system was made by Ghosh [4], and his work was later used and slightly modified by Miettinen [5] for theoretical assessment of the Cu-rich corner of the Cu–Ni–Sn system. These assessments

---

Dedicated to Professor H. Ipsen on the occasion of his 65th birthday.

---

A. Zemanova · A. Kroupa (✉)  
Institute of Physics of Materials, Academy of Sciences  
of the Czech Republic, Zizkova 22, 616 62 Brno,  
Czech Republic  
e-mail: kroupa@ipm.cz

A. Zemanova  
e-mail: zemanova@ipm.cz

A. Dinsdale  
National Physical Laboratory, Teddington, UK

were later reworked by Liu et al. [6] to improve the theoretical description of the fcc and liquid phases, because there were problems when extrapolating these phases to metastable regions.

All the previous theoretical assessments discussed above [4–6] reproduced well the experimental results which had been obtained at the time of the assessment. Liu [6] mainly worked with phase data (liquidus temperatures and temperatures of invariant reactions) from Mikulas et al. [7] and Heumann [8]. Mikulas [7] carried out a very detailed study of the liquidus in the Ni–Sn system. He proposed completely different phase boundaries in the region of intermetallic phases. He suggested the existence of a stable  $\text{Ni}_4\text{Sn}$  phase and the existence of two liquid miscibility gaps. None of these features was confirmed later by Heumann [8], who studied also the liquidus and invariant temperatures in the region between 20 and 70 wt% Ni. In his assessment, Liu [6] used data from Ref. [8] together with the liquidus temperatures from the Sn-rich and Ni-rich regions and (fcc\_Ni) solidus temperatures from Ref. [7]. The invariant temperatures were taken from Ref. [9].

Schmetterer et al. [3], however, performed a very detailed experimental study of the Ni–Sn system. They found significant discrepancies among measured values of most of the invariant temperatures in comparison with Ref. [9] and also identified very complex behaviour of the low-temperature  $\text{Ni}_3\text{Sn}_2$  phase. The calculated phase diagrams assessed by Liu [6] and the diagram established by Schmetterer [3] are shown in Figs. 1 and 2.

The work of Schmetterer was therefore used as the basic source of experimental phase data for the reassessment,

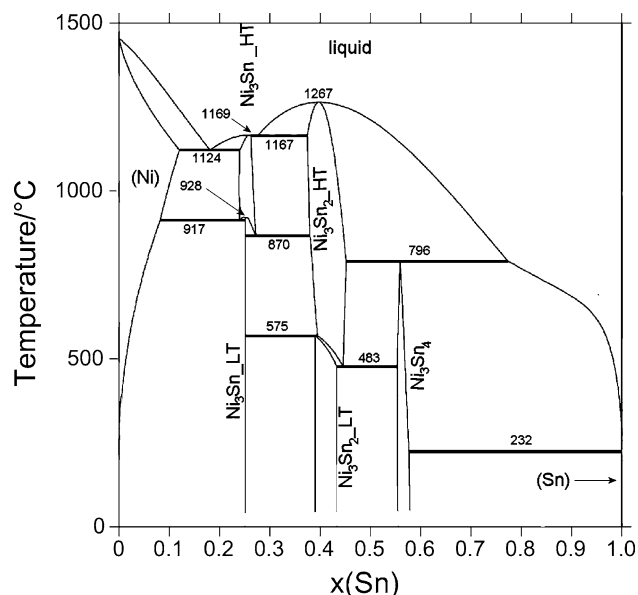


**Fig. 1** Previously assessed Ni–Sn phase diagram (from Liu et al. [6])

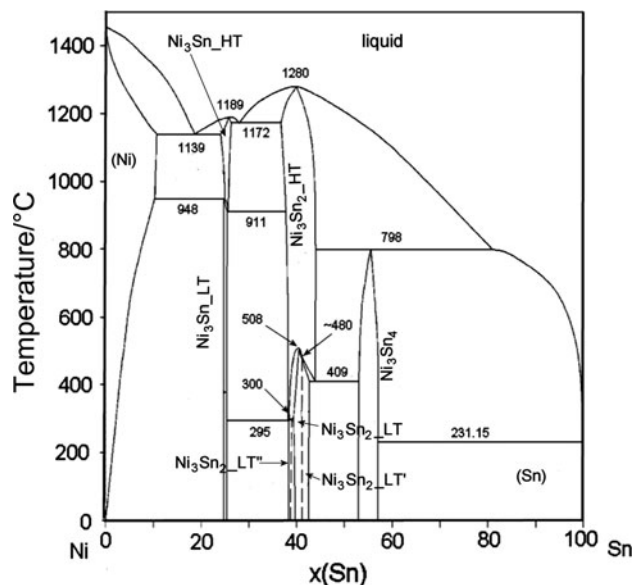


**Fig. 2** Ni–Sn phase diagram according to Schmetterer et al. [3]

together with additional experimental data from Ref. [10] (and from Mishra R and Ipsier H; personal communication). Gourlay et al. [10] studied the ternary Cu–Ni–Sn system in the Sn-rich corner and determined the eutectic concentration of liquid in the binary system.

Similarly, Mishra R and Ipsier H (personal communication) studied the Ni–Sb–Sn system for 80 and 85 at.% Sn and determined the transition temperature for the binary Ni–Sn system in this region to be 800 °C for 80 at.% Sn and 780 °C for 85 at.% Sn. Measurements of the thermodynamic properties [11–18] examined by Liu et al. [6] in their assessment were also used to verify the results of the theoretical reassessment.

**Table 1** Crystallographic structures of phases present in the Ni–Sn system

Common name	Database name	Strukturbericht designation	Pearson symbol
Liquid	LIQUID		
(Ni)	FCC_A1	A1	<i>cF4</i>
( $\beta$ Sn)	BCT_A5	A5	<i>tI4</i>
( $\alpha$ Sn)	DIAMOND_A4	A4	<i>cF8</i>
$\text{Ni}_3\text{Sn}_{\text{HT}}$	BCC_A2 <sup>a</sup>	<i>DO</i> <sub>3</sub>	<i>cF16</i>
$\text{Ni}_3\text{Sn}_{\text{LT}}$	NI3SN_LT	<i>DO</i> <sub>19</sub>	<i>hP8</i>
$\text{Ni}_3\text{Sn}_2\text{-LT(LT}', \text{LT}'')$	NIAS_TYPE	–	<i>oP20</i>
$\text{Ni}_3\text{Sn}_2\text{-HT}$	–	–	<i>hP6</i>
$\text{Ni}_3\text{Sn}_4$	NI3SN4	–	<i>mC14</i>

<sup>a</sup> Phase information (common name, Strukturbericht designation, and Pearson symbol) are given for the real  $\text{Ni}_3\text{Sn}_{\text{HT}}$  phase

**Table 2** Thermodynamic data for the Ni–Sn system, optimized in this study

Ni <sub>3</sub> Sn <sub>4</sub> HT, modelled as BCC_A2 - 2 sublattices (Ni,Sn) <sub>1</sub> (Va) <sub>3</sub>	
${}^0L_{\text{Ni,Sn:Va}}^{\text{BCC\_A2}}$	$= +2369+43.736*T$
${}^1L_{\text{Ni,Sn:Va}}^{\text{BCC\_A2}}$	$= -654762.56+63.272352*T$
${}^2L_{\text{Ni,Sn:Va}}^{\text{BCC\_A2}}$	$= +689895.17-94.74087*T$
(βSn)/BCT_A5, 1 sublattice (Ni,Sn) <sub>1</sub>	
${}^0L_{\text{Ni,Sn}}^{\text{BCT\_A5}}$	$= -21500$
(αSn)/DIAMOND_A4, 1 sublattice (Sn) <sub>1</sub>	
$G_{\text{Sn}}^{\text{DIAMOND\_A4}}$	$= 100.00 < T < 298.14: -9579.608+114.007785*T-22.972*T*\ln(T)$
	$-0.00813975*T**2 + 2.7288E-06*T**3+25615*T*(-1)$ [19]
	$298.14 < T < 800.00: -9063.001+104.84654*T-21.5750771*T*\ln(T)-0.008575282*T**2$
	$+1.784447E-06*T**3-2544*T*(-1)$
	$800.00 < T < 3000.00: -10909.351+147.396535*T-28.4512*T*\ln(T)$
(Ni)/FCC_A1, 2 sublattices (Ni,Sn) <sub>1</sub> (Va) <sub>1</sub>	
${}^0L_{\text{Ni,Sn:Va}}^{\text{FCC\_A1}}$	$= -69507.35+74.5697727*T-8.0319551*T*\ln(T)$
${}^1L_{\text{Ni,Sn:Va}}^{\text{FCC\_A1}}$	$= -12395.19$
${}^0T_{\text{C}}^{\text{FCC\_A1}}$	$= -6000$ [6]
${}^1T_{\text{C}}^{\text{FCC\_A1}}$	$= 3000$ [6]
${}^0B_{\text{magn}}^{\text{FCC\_A1}}$	$= -6.8002$ [6]
${}^1B_{\text{magn}}^{\text{FCC\_A1}}$	$= 4.3689$ [6]
Liquid/LIQUID, 1 sublattice (Ni,Sn) <sub>1</sub>	
${}^0L_{\text{Ni,Sn}}^{\text{liquid}}$	$= -104602.87+197.8089*T-21.6959*T*\ln(T)$
${}^1L_{\text{Ni,Sn}}^{\text{liquid}}$	$= -30772.17+52.5528*T-7.56094*T*\ln(T)$
${}^2L_{\text{Ni,Sn}}^{\text{liquid}}$	$= 6582.31$
Ni <sub>3</sub> Sn <sub>4</sub> /NI3SN4, 3 sublattices (Ni) <sub>0.25</sub> (Ni,Sn) <sub>0.25</sub> (Sn) <sub>0.5</sub>	
${}^0G_{\text{Ni:Sn}}^{\text{Ni3Sn4}}$	$= -25078.56+4.291*T+.5*{}^0G_{\text{Ni}}^{\text{HSER}}+.5*{}^0G_{\text{Sn}}^{\text{HSER}}$
${}^0G_{\text{Ni:Sn:Sn}}^{\text{Ni3Sn4}}$	$= +7613.24+8.749*T+.25*{}^0G_{\text{Ni}}^{\text{HSER}}+.75*{}^0G_{\text{Sn}}^{\text{HSER}}$ [6]
${}^0L_{\text{Ni:Sn:Sn}}^{\text{Ni3Sn4}}$	$= -52928.16$
Ni <sub>3</sub> Sn <sub>2</sub> LT/NI3SN_LT, 2 sublattices (Ni,Sn) <sub>0.75</sub> (Ni,Sn) <sub>0.25</sub>	
${}^0G_{\text{Ni:Ni}}^{\text{Ni3Sn2LT}}$	$= +6300+{}^0G_{\text{Ni}}^{\text{HSER}}$
${}^0G_{\text{Sn:Ni}}^{\text{Ni3Sn2LT}}$	$= +5000+.25*{}^0G_{\text{Ni}}^{\text{HSER}}+.75*{}^0G_{\text{Sn}}^{\text{HSER}}$
${}^0G_{\text{Ni:Sn}}^{\text{Ni3Sn2LT}}$	$= -28408+7.0009*T+.75*{}^0G_{\text{Ni}}^{\text{HSER}}+.25*{}^0G_{\text{Sn}}^{\text{HSER}}$
${}^0G_{\text{Sn:Sn}}^{\text{Ni3Sn2LT}}$	$= +5000+{}^0G_{\text{Sn}}^{\text{HSER}}$
Ni <sub>3</sub> Sn <sub>2</sub> LT',LT'', Ni <sub>3</sub> Sn <sub>2</sub> HT, modelled as one phases NIAS_TYPE, 3 sublattices (Ni,Va) <sub>1</sub> (Ni,Va) <sub>1</sub> (Ni,Sn) <sub>1</sub>	
${}^0G_{\text{Ni:Ni:Ni}}^{\text{NIAS\_TYPE}}$	$= +31637.299+355.176064*T-66.288*T*\ln(T)-.0145221*T**2$
${}^0G_{\text{Va:Ni:Ni}}^{\text{NIAS\_TYPE}}$	$= +21091.532+236.784043*T-44.192*T*\ln(T)-.0096814*T**2$
${}^0G_{\text{Ni:Va:Ni}}^{\text{NIAS\_TYPE}}$	$= +21091.532+236.784043*T-44.192*T*\ln(T)-.0096814*T**2$
${}^0G_{\text{Va:Va:Ni}}^{\text{NIAS\_TYPE}}$	$= +10545.766+118.58688*T-22.096*T*\ln(T)-.0048407*T**2$
${}^0G_{\text{Ni:Ni:Sn}}^{\text{NIAS\_TYPE}}$	$= +2*{}^0G_{\text{Ni}}^{\text{HSER}}+{}^0G_{\text{Sn}}^{\text{HSER}}-83734.818+14.6888165*T$
${}^0G_{\text{Va:Ni:Sn}}^{\text{NIAS\_TYPE}}$	$= +5000+{}^0G_{\text{Sn}}^{\text{HSER}}+{}^0G_{\text{Ni}}^{\text{HSER}}$
${}^0G_{\text{Ni:Va:Sn}}^{\text{NIAS\_TYPE}}$	$= +{}^0G_{\text{Ni}}^{\text{HSER}}+{}^0G_{\text{Sn}}^{\text{HSER}}-52177.98+10.774*T$
${}^0G_{\text{Va:Va:Sn}}^{\text{NIAS\_TYPE}}$	$= +20000+{}^0G_{\text{Sn}}^{\text{HSER}}$
${}^0L_{\text{Ni:Ni:Va:Sn}}^{\text{NIAS\_TYPE}}$	$= -9784.4-12.385*T$
${}^1L_{\text{Ni:Ni:Va:Sn}}^{\text{NIAS\_TYPE}}$	$= 12000$

Values in J/mol, the reference state is SER. The common names and database names are shown

## Results and discussion

The crystallographic structures of all the phases present in the system and critically assessed thermodynamic data are presented in Tables 1 and 2. The data for the pure elements Ni and Sn for the different phases are taken from Ref. [19] and ThermoCalc software was used for the optimisation. The calculated phase diagram of the Ni–Sn system is shown in Fig. 3. Experimental phase data from Refs. [3] and [7] and from Mishra R and Ipsen H (personal communication)

are compared with results from theoretical calculations in Fig. 4, and details of the phase diagram in the region close to congruent melting of the Ni<sub>3</sub>Sn<sub>2</sub> phase is shown in Fig. 5. The data from Ref. [7] were not used during the assessment, only for the final verification of the calculations. The agreement between the calculations and experiments is very good and all the important transition temperatures are well reproduced by the assessment (Table 3).

Comparison of the experimental enthalpy of mixing of liquid Ni–Sn alloys from Refs. [9–11] with our calculations

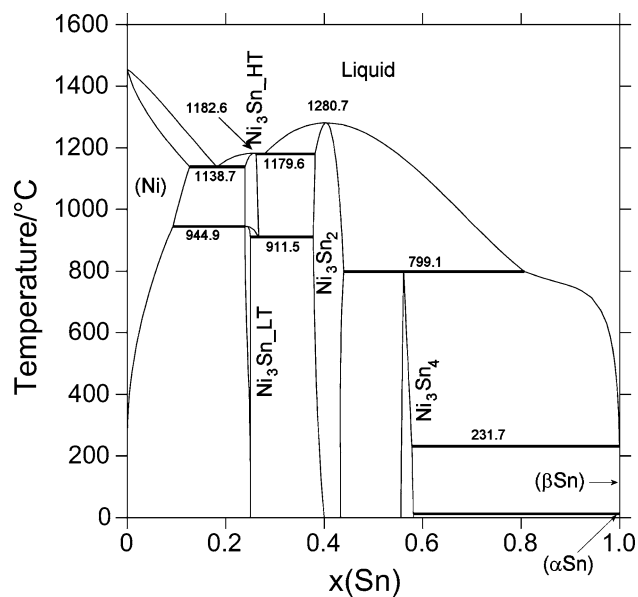


**Fig. 3** Calculated phase diagram of the Ni–Sn system

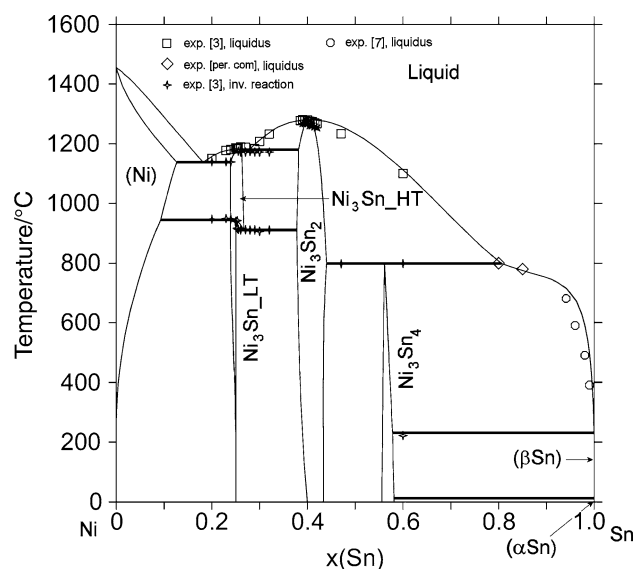


**Fig. 4** Comparison of the calculated Ni–Sn phase diagram with experimental results from Ref. [3] and from Mishra R and Ipsier H (personal communication)  $\diamond$

and those of Liu [6] is shown in Fig. 6, and comparison of the experimental enthalpy of formation for the solid alloys from Refs. [15] and [18] and with calculations is shown in Fig. 7. The calculated activities from our work, from the assessment of Liu et al. [6], and the experimental results of Eremenko et al. [14] are compared in Fig. 8.

Agreement with the thermodynamic measurements [11–18] used by Ref. [6] is also very good for the enthalpies of mixing in the liquid and for the activities of Sn. There is slight disagreement for the enthalpies of

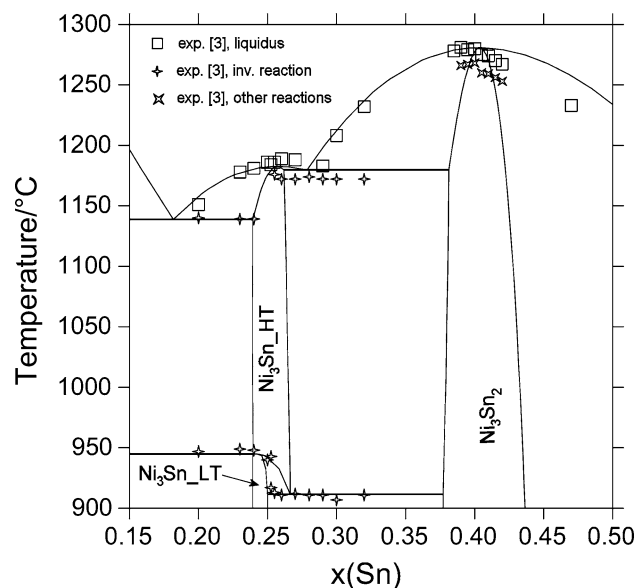


**Fig. 5** Comparison of detail of the calculated Ni–Sn phase diagram with experimental results from Ref. [3]

formation, mainly for  $\text{Ni}_3\text{Sn}_2$ , similar to that found by Liu [6] and Ghosh [4]. With regard to the small amount of new experimental data, we assume this is acceptable.

### Thermodynamic modelling

Basic information about the phase modelling using the CALPHAD method is given in this section. A detailed description of the method can be found in the book by Lukas et al. [20].

#### Modelling of liquid and solid solution phases *bct\_A5* and *fcc\_A1*

The *bct\_A5* phase (Sn solid solution) and the liquid phase were modelled in terms of a standard substitutional model with one sublattice.

The molar Gibbs energy of a solution phase  $\phi$  can be regarded as the sum of different contributions:

$$G_m^\phi = G_{\text{ref}}^\phi + G_{\text{id}}^\phi + G_E^\phi + G_{\text{mag}}^\phi + G_P^\phi + \dots \quad (1)$$

where  $G_{\text{ref}}^\phi$  is the molar Gibbs energy of the weighted sum of the system constituents  $i$  (elements, species, compounds, etc.) in the crystallographic structure corresponding to the phase  $\phi$  relative to the chosen reference state (typically the stable element reference state, SER):

$$G_{\text{ref}}^\phi = \sum_{i=1}^n x_i \cdot G_i^\phi \quad (2)$$

and its temperature dependence is given by:

**Table 3** Table of transition temperatures (experimental results from Ref. [3])

$T_{\text{exp}}/^\circ\text{C}$	$T_{\text{calc}}/^\circ\text{C}$ (this work)	$T_{\text{calc}}/^\circ\text{C}$ (from Ref. [6])	Phases			Composition/ $x_{\text{Sn}}$		
n.a.	1,455	1,455	Liquid	Ni		0.000	0.000	
1,280	1,280.8	1,267	Liquid	$\text{Ni}_3\text{Sn}_2$		0.401	0.401	
1,189	1,182.6	1,169	Liquid	$\text{Ni}_3\text{Sn}_{\text{HT}}$		0.259	0.259	
1,172	1,179.6	1,167	$\text{Ni}_3\text{Sn}_{\text{HT}}$	Liquid	$\text{Ni}_3\text{Sn}_2$	0.262	0.278	0.384
1,139	1,138.7	1,124	Ni	Liquid	$\text{Ni}_3\text{Sn}_{\text{HT}}$	0.126	0.182	0.239
n.a.	945.0	928	$\text{Ni}_3\text{Sn}_{\text{HT}}$	$\text{Ni}_3\text{Sn}_{\text{LT}}$		0.240	0.240	
948	944.9	917	Ni	$\text{Ni}_3\text{Sn}_{\text{LT}}$	$\text{Ni}_3\text{Sn}_{\text{HT}}$	0.093	0.239	0.240
911	911.1	870	$\text{Ni}_3\text{Sn}_{\text{LT}}$	$\text{Ni}_3\text{Sn}_{\text{HT}}$	$\text{Ni}_3\text{Sn}_2$	0.250	0.266	0.378
798	798.0	796	$\text{Ni}_3\text{Sn}_2$	$\text{Ni}_3\text{Sn}_4$	Liquid	0.432	0.561	0.794
n.a.	231.9	232	Liquid	Sn		1.000	1.000	
213.2	231.7	232	$\text{Ni}_3\text{Sn}_4$	Liquid	$\beta\text{Sn}$	0.578	0.999	0.100
n.a.	13.1	n.a.	$\text{Ni}_3\text{Sn}_4$	$\beta\text{Sn}$	$\alpha\text{Sn}$	0.580	1.000	1.000
n.a.	13.0	n.a.	$\beta\text{Sn}$	$\alpha\text{Sn}$		1.000	1.000	

n.a., not available

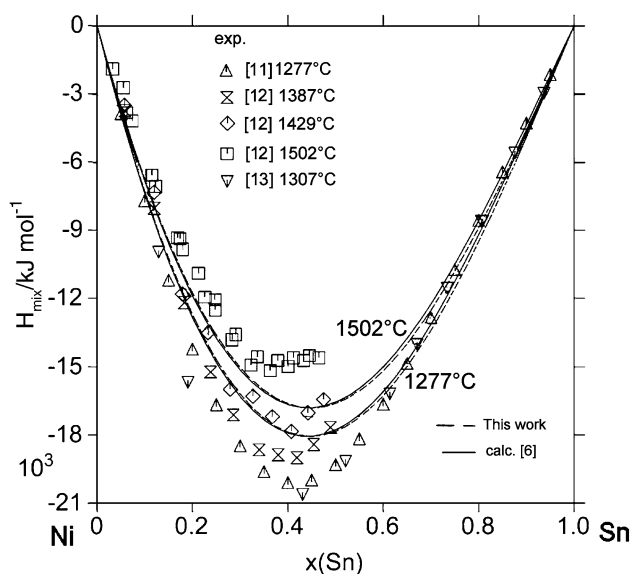


**Fig. 6** Comparison of calculated enthalpy of mixing in liquid Ni–Sn for temperatures 1,277 and 1,502 °C (from Ref. [6] and this work) with experimentally measured values from Refs. [11–13] (standard states liquid Ni and Sn)

$$G(T) = a + bT + cT\ln(T) + \sum_i d_i T^n \quad (3)$$

where a–d<sub>i</sub> are adjustable coefficients.

The contribution to the Gibbs energy from ideal random mixing of the constituents in the crystal lattice or in the liquid, denoted  $G_{\text{id}}^\phi$ , is defined as ideal mixing:

$$G_{\text{id}}^\phi = RT \sum_{i=1}^n x_i \cdot \ln(x_i) \quad (4)$$

for an *n*-constituent system.

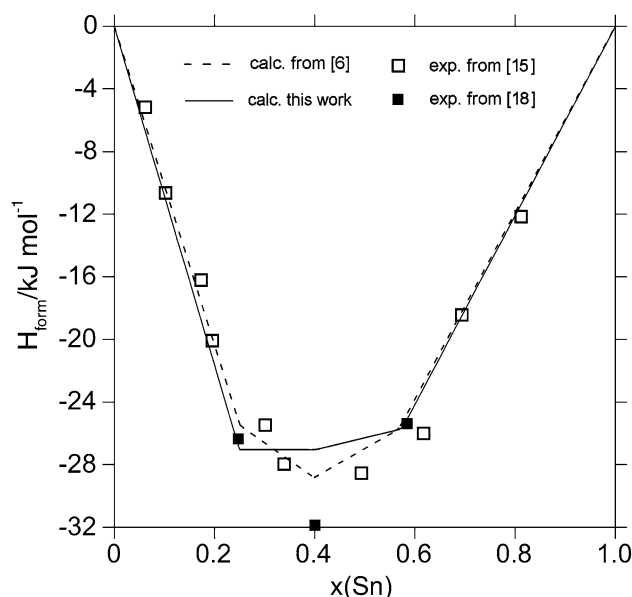


**Fig. 7** Comparison of calculated enthalpy of formation of solid alloys for the temperature 25 °C (from Ref. [6] and this work) with experimentally measured values from Refs. [15] and [18] (standard states fcc\_Ni and bct\_Sn)

The Gibbs energy, which describes the effect of non-ideal mixing behaviour on the thermodynamic properties of a solution phase, is given by Redlich–Kister formalism [21]:

$$G_E^\phi = \sum_{\substack{i,j=1 \\ i \neq j}}^n x_i x_j \sum_{z=0}^m {}^z L (x_i - x_j)^z \quad (5)$$

where the temperature-dependent interaction variables, describing the mutual interaction between constituents *i*

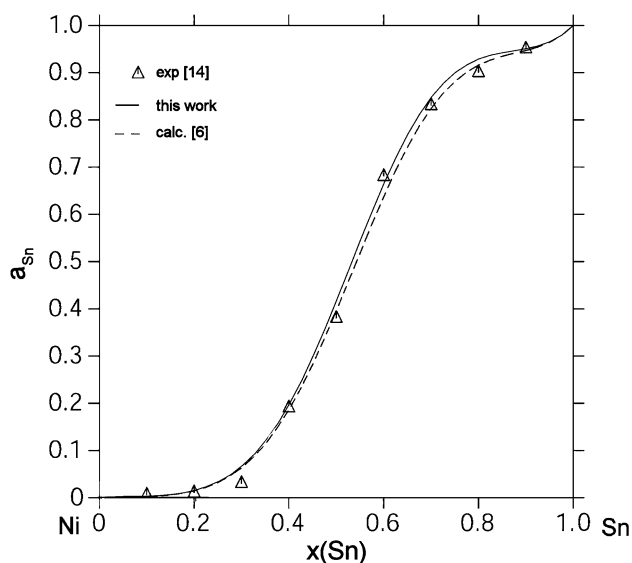


**Fig. 8** Comparison of the calculated activity of Sn in liquid Ni–Sn for the temperature 1,300 °C (from Ref. [6] and this work) with experimentally measured values from Ref. [14] (standard state liquid Sn)

and  $j$ , are denoted  ${}^zL$ . The temperature dependence of the interaction variable is usually defined as:

$$L(T) = a + bT + cT \ln(T) \quad (6)$$

The fcc\_A1 phase (Ni solid solution) is formally modelled as an interstitial solid solution, using two sublattices, one occupied by metal atoms the other by interstitial atoms and structural vacancies. There are no interstitial elements in the Ni–Sn system, nevertheless this model was selected to maintain consistency with other assessments in which interstitials have been included (e.g., austenite in steels). In the fcc phase of the Ni–Sn system the second sublattice of the thermodynamic model contains only vacancies and the model essentially corresponds to the above mentioned substitutional model.

#### Modelling of intermetallic phases

##### Ni<sub>3</sub>Sn<sub>2</sub> phase

The low-temperature Ni<sub>3</sub>Sn phase has the  $D0_{19}$  type structure (Pearson symbol  $hP8$ ) and is modelled by using two sublattices with full miscibility of both elements (Ni,Sn)<sub>0.75</sub> and (Ni,Sn)<sub>0.25</sub>.

The  $G_{\text{ref}}^{\phi}$  for such a model is given by:

$$G_{\text{ref}}^{\phi} = \sum y_i^1 \cdot y_j^2 G_{(ij)}, i, j = \text{Ni, Sn} \quad (7)$$

where the  $y$  terms are the site fractions of each constituent in the relevant sublattices, 1 and 2. The term  $G_{(ij)}$  is the Gibbs energy of formation of “virtual compound”  $ij$ , or the Gibbs energy of pure element  $i$  in the given crystallographic structure if both sublattices are occupied by the

same component. Typically only few of these compounds exist in reality, but data for all the relevant end members are needed for the modelling.

The ideal mixing term is given by:

$$G_{\text{id}}^{\phi} = \sum_{p=1}^2 f_p \cdot \sum_{i=1}^2 y_i^p \cdot \ln(y_i^p) \quad (8)$$

where  $f_p$  is the stoichiometric coefficient for a given sublattice and the second sum describes the effect of ideal mixing within sublattice  $p$ . The excess contribution is now given by:

$$G_E^{\phi} = \sum y_i^1 \cdot y_j^1 \cdot y_k^2 L_{(i,j;k)} + \sum y_i^1 \cdot y_k^2 \cdot y_m^2 L_{(i;k,m)} \quad (9)$$

where:

$$L_{(i,j;k)} = \sum_z {}^zL_{(i,j;k)} \cdot (y_i - y_j)^z \quad (10)$$

The term  $L_{(i,j;k)}$  describes the mutual interaction of constituents  $i$  and  $j$  in the first sublattice, when the second sublattice is fully occupied by constituent  $k$ . This description can be extended in the same way to any number of sublattices.

##### Ni<sub>3</sub>Sn<sub>2</sub> phase

A high-temperature Ni<sub>3</sub>Sn phase with the  $D0_3$  structure has been observed in the Ni–Sn system. Here some simplifications of the observed crystallography of the phase and of the changes of the thermodynamic models used in previous assessments were made. This assessment is part of the European projects COST531 [22] and MP0602 [23], in which creation of consistent thermodynamic databases for lead-free soldering and high-temperature lead-free soldering was a key objective.

In the ternary Cu–Ni–Sn system, a continuous solubility region is observed between the high-temperature BCC\_A2 phase originating in the Cu–Sn binary and this Ni<sub>3</sub>Sn<sub>2</sub> phase. To maintain consistency between the thermodynamic data for the different binary systems in these databases (SOLDERS [24] and COST MP0602 [23]), it was necessary to unify the models used for both phases. Otherwise, it would not be possible to model that region as a single phase. It was decided to reassess the Ni<sub>3</sub>Sn<sub>2</sub> phase as having the BCC\_A2 structure to be consistent with the simplified model selected for the relevant phase in the Cu–Sn system in the SOLDERS database [24].

##### Ni<sub>3</sub>Sn<sub>2</sub> phase

The family of Ni<sub>3</sub>Sn<sub>2</sub> phases (Ni<sub>3</sub>Sn<sub>2</sub>-HT, Ni<sub>3</sub>Sn<sub>2</sub>-LT, Ni<sub>3</sub>Sn<sub>2</sub>-LT', Ni<sub>3</sub>Sn<sub>2</sub>-LT'') [3] was modelled as a single phase, as the phase relationships between them are quite complex and the transition temperatures and concentration regions of individual phases are not completely described.

Also, because complete solubility was found experimentally in several ternary systems between the phases with crystallographic structures *hP4* (NiAs prototype) and *hP6* (Ni<sub>3</sub>Sn<sub>2</sub>-HT phase, Ni<sub>2</sub>In prototype), the Ni<sub>3</sub>Sn<sub>2</sub> family of phases was modelled by using a three-sublattice model to maintain general consistency in the above mentioned databases. The model, reflecting the crystallography of the phase *hP6*, can be described as (Ni,Va)<sub>1</sub>(Ni,Va)<sub>1</sub>(Ni,Sn)<sub>1</sub>.

#### Phase Ni<sub>3</sub>Sn<sub>4</sub>

The three-sublattice model reflecting the crystallography of the phase can be described as (Ni)<sub>0.25</sub>(Ni,Sn)<sub>0.25</sub>(Sn)<sub>0.5</sub>.

## Conclusions

The CALPHAD method was used to reassess the phase diagram and thermodynamic properties of the Ni–Sn system taking into account the latest experimental results from Ref. [3]. The thermodynamic description of Ref. [6] was used as the initial basis for the work. The solid solution phases were modified slightly from the original assessment, and the thermodynamic descriptions of the intermetallic phases have been changed substantially. Reassessment of the data for the system was necessary because of new experimental work which resulted in significant changes to invariant temperatures. Furthermore the models used for description of the intermetallic phases were changed, for compatibility with the SOLDERS [24] database.

The agreement between the experimental results and the new theoretical calculations is very good, both with regard to the new experimental phase diagram results from Ref. [3] and measurements of the thermodynamic properties [11–18].

**Acknowledgments** This work was supported by the COST MP0602 action and the research project LD11024. The authors wish to express their thanks to Dr A. Watson, Professor J Vrestal, and Professor P. Broz for their fruitful help during the development of the thermodynamic database.

## References

- Kodentsov A (2010) On the merits of transient liquid phase bonding as a substitute for soldering with High-Pb alloys. Presented at the 139th TMS Annual Meeting, February 14–18, 2010, Seattle, USA
- Sosnowska KK, Pawelkiewicz M, Janczak-Rusch J, Spolenak R (2012) Acta Mater (submitted)
- Schmetterer C, Flandorfer H, Richter KW, Saeed U, Kauffman M, Roussel P, Ipser H (2007) Intermetallics 15:869
- Ghosh G (1999) Metall Mater Trans 30A:1481
- Miettinen J (2003) CALPHAD 27:309
- Liu HS, Mang J, Jin ZP (2004) CALPHAD 28:363
- Mikulas W, Thomassen L, Upthegrove C (1937) Trans AIME 124:111
- Heumann T (1943) Z Metallkd 35:206
- Nash P, Nash A (1985) Bull Alloy Phase Diagr 6:350
- Gourlay CM, Nogita K, Read J, Dahle AK (2010) J Electron Mater 39:56
- Haddad R, Gaune-Escard M, Bros JP, Havlicek A, Hayer E, Komarek KL (1997) J Alloys Compd 247:82
- Luck R, Tomiska J, Predel B (1988) Z Metallkd 79:345
- Pool MJ, Arpschhofen I, Predel B, Schultheiss B (1979) Z Metallkd 70:656
- Eremenko VN, Lukashenko GM, Pritula VL (1971) Russ J Phys Chem 45:1131
- Korber F, Oelson W (1937) Mitt Kaiser Wilhelm Inst F Eisenforsch 19:209
- Dannohl H-D, Lukas HL (1974) Z Metallkd 65:642
- Predel B, Ruge H (1972) Thermochem Acta 3:411
- Predel B, Vogelbein W (1979) Thermochem Acta 30:205
- SGTE Unary database ver. 4.4. <http://www.sgte.org/>
- Lukas HL, Fries SG, Sundman B (2007) Computational thermodynamics—the Calphad method. Cambridge University Press, London
- Redlich O, Kister A (1948) Ind Eng Chem 40:345
- Ipser H, COST Action 531—Lead-free Solder materials (End date: March 2007). [http://www.cost.esf.org/domains\\_actions/mpns/Actions/Lead-free\\_Solder\\_Materials](http://www.cost.esf.org/domains_actions/mpns/Actions/Lead-free_Solder_Materials)
- Kroupa A, COST Action MP0602—Advanced Solder materials for high temperature application (HISOLD). [http://w3.cost.esf.org/index.php?id=248&action\\_number=MP0602](http://w3.cost.esf.org/index.php?id=248&action_number=MP0602)
- Dinsdale AT, Watson A, Kroupa A, Vrestal J, Zemanova A, Vizdal J (2008) Version 3.0 of the SOLDERS Database for Lead Free Solders. <http://resource.npl.co.uk/mtdata/soldersdatabase.htm>